J|A|C|S
ARTICLES
Published on Web 03/18/2003

Mechanism of the Stille Reaction Catalyzed by Palladium Ligated to Arsine Ligand: PhPdI(AsPh$_3$)(DMF) Is the Species Reacting with Vinylstannane in DMF

Christian Amatore,*,† Ali A. Bahsoun,† Anny Jutand,*,† Gilbert Meyer,†
Alexandre Ndedi Ntepe,† and Louis Ricard‡

Contribution from the Ecole Normale Supérieure, Département de Chimie, UMR CNRS-ENS-UPMC 8640, 24 Rue Lhomond, 75231 Paris Cedex 5, France, and Ecole Polytechnique, DCPH, UMR CNRS 7653, 91128 Palaiseau, France

Received April 5, 2002

Abstract: The kinetics of the reaction of PhPdI(AsPh$_3$)$_2$ (formed via the fast oxidative addition of PhI with Pd^0(AsPh$_3$)$_2$) with a vinyl stannane CH$_2$═CH−Sn(*n*-Bu)$_3$ has been investigated in DMF. This reaction (usually called transmetalation step) is the prototype of the rate determining second step of the catalytic cycle of Stille reactions. It is established here that the transmetalation proceeds through PhPdI(AsPh$_3$)(DMF), generated by the dissociation of one ligand AsPh$_3$ from PhPdI(AsPh$_3$)$_2$. PhPdI(AsPh$_3$)(DMF) is the reactive species, which leads to styrene through its reaction with CH$_2$═CH−SnBu$_3$. Consequently, in DMF, the overall nucleophilic attack mainly proceeds via a mechanism involving PhPdI(AsPh$_3$)(DMF) as the central reactive complex and not PhPdI(AsPh$_3$)$_2$. The dimer [Ph$_2$Pd$_2$(μ^2-I)$_2$(AsPh$_3$)$_2$] has been independently synthesized and characterized by its X-ray structure. In DMF, this dimer dissociates quantitatively into PhPdI(AsPh$_3$)(DMF), which reacts with CH$_2$═CH−SnBu$_3$. The rate constant for the reaction of PhPdI(AsPh$_3$)(DMF) with CH$_2$═CH−SnBu$_3$ has been determined in DMF for each situation and was found to be comparable.

Introduction

The mechanism of the Palladium-catalyzed Stille reaction[1] (cross coupling of aryl halides and organostannanes derivatives, eq 1) has been widely investigated.[1−8] The original mechanism proposed by Stille,[1a] in the case of monodentate ligand L, included four steps: oxidative addition, transmetalation, trans−cis isomerization and reductive elimination (Scheme 1), involving saturated 16-electron aryl-Pd^{II} complexes, all ligated by two phosphine ligands.

Scheme 1. Initial Mechanism

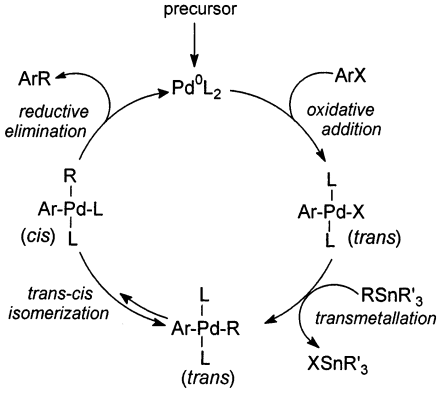

$$\mathrm{ArX} + \mathrm{RSnR'_3} \xrightarrow{\mathrm{Pd}} \mathrm{ArR} + \mathrm{XSnR'_3} \qquad (1)$$

This initial mechanism has been progressively modified to rationalize the effect of ligands (ex: AsPh$_3$ vs PPh$_3$) on the efficiency of catalytic reactions.[2−4] Much attention has been paid to the transmetalation step, which was very early identified as the rate determining step.[2−4b] Because this step is retarded by excess ligand,[2−4b] aryl-Pd^{II} complexes, ligated by only one

* Dedicated to Professor Marc Julia on the occasion of his 80th birthday.
† Ecole Normale Supérieure.
‡ Ecole Polytechnique.

(1) (a) Stille, J. K. *Angew. Chem., Int. Ed. Engl.* **1986**, *25*, 508−524. (b) Farina, V.; Krishnamurthy, V.; Scott, W. J. *The Stille Reaction in Organic Reactions*; Wiley: New York, 1997, Vol. *50*, p 1.
(2) Louie, J.; Hartwig, J. F. *J. Am. Chem. Soc.* **1995**, *117*, 11 598−11 599.
(3) (a) Farina, V.; Krisnan, B. *J. Am. Chem. Soc.* **1991**, *113*, 9585−9595. (b) Farina, V.; Roth, G. P. *Recent Advances in the Stille Reaction* In *Adv. Metalorg. Chem.* **1996**, *5*, 1−53.
(4) (a) Casado, A. L.; Espinet, P. *Organometallics* **1998**, *17*, 7, 954−959. (b) Casado, A. L.; Espinet, P. *J. Am. Chem. Soc.* **1998**, *120*, 8978−8985.
(5) For the mechanism of Stille reactions from aryl triflates, see ref 3 and (a) Farina, V.; Krisnan, B.; Marshall, D. R.; Roth, G. P. *J. Org. Chem.* **1993**, *58*, 5434−5444. (b) Casado, A. L.; Espinet, P.; Gallego, A. *J. Am. Chem. Soc.* **2000**, *122*, 11 771−11 782. (c) Casado, A. L.; Espinet P.; Gallego, A. M.; Martinez-Ilarduya, J. M. *J. Chem. Soc. Chem. Comm.* **2001**, *120*, 339−340.
(6) Ricci, A.; Angelucci, F.; Bassetti, M.; Lo Sterzo, C. *J. Am. Chem. Soc.* **2002**, *124*, 1060−1071.
(7) Mateo, C.; Fernández-Rivas, C.; Cárdenas, D. J.; Echavarren, A. M. *Organometallics* **1998**, *17*, 7, 3661−3669.
(8) Amatore, C.; Bucaille, A.; Fuxa, A.; Jutand, A.; Meyer, G.; Ndedi Ntepe, A. *Chem. Eur. J.* **2001**, 2134−2142.

10.1021/ja0204978 CCC: $25.00

Scheme 2. Updated Mechanism (L = $AsPh_3$)[3a,4b]

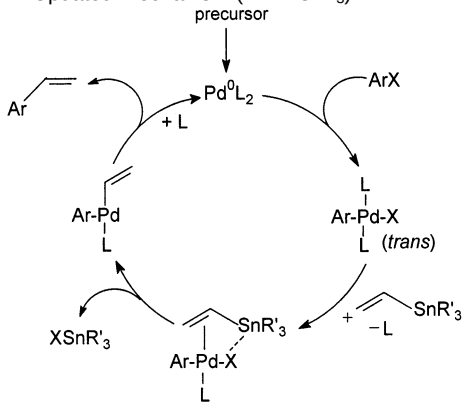

Scheme 3. Mechanism of the Oxidative Addition in DMF[8]

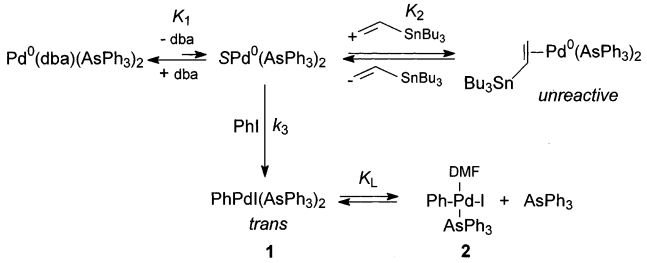

ligand L, have been proposed as key intermediates in the transmetalation and henceforth in the reductive-elimination step (Scheme 2).[2,3,4b,9]

In the course of our investigation on the effect of the arsine ligand $AsPh_3$ on the rate of the oxidative addition of PhI, which is the first step of a catalytic reaction between PhI and the tri-*n*-butyl(vinyl)tin in DMF (eq 2), we established that $CH_2{=}CH{-}SnBu_3$ coordinates the active *S*$Pd^0(AsPh_3)_2$ complex prior to its oxidative addition to PhI, thereby leading to the unreactive (η^2-$CH_2{=}CH{-}SnBu_3$)$Pd^0(AsPh_3)_2$ species (Scheme 3).[8]

$$\mathrm{PhI + CH_2{=}CH\text{-}SnBu_3 \xrightarrow[DMF]{Pd^0(dba)_2 + 2AsPh_3} PhCH{=}CH_2 + ISnBu_3} \qquad (2)$$

Due to this side route, which stores part of the catalytic charge under an unreactive form, the oxidative addition of PhI is slower when performed in the presence of the nucleophile, i.e., under the conditions which prevail in a real catalytic reaction. The complex $PhPdI(AsPh_3)_2$, formed after oxidative addition to *S*$Pd^0(AsPh_3)_2$, was shown to dissociate one $AsPh_3$ ligand in chloroform and DMF.[8] This decomplexation was observed to proceed in appreciable extents in both solvents. This led to the concomitant formation of a new $PhPd^{II}$ moiety ligated by only one $AsPh_3$, which was assigned to be $PhPdI(AsPh_3)$(*S*) complex[8] (Scheme 3) upon following the original proposal of Farina in THF[3] (the structure of the complex in chloroform will be discussed at the very end of this paper). In DMF, the equilibrium constant $K_L = [PhPdI(AsPh_3)(DMF)][AsPh_3]/[PhPdI(AsPh_3)_2]$ was determined: $K_L = 3.1 \times 10^{-4}$ M at 25 °C,[8] a value which is not very different from that determined by Farina and Krishnan ($K_L = 8.6 \times 10^{-4}$ M) on the basis of their investigation of the kinetics of the catalytic reaction 2 in THF at 50 °C.[3]

We wish to report here new investigations on the kinetics of the transmetalation step performed from $PhPdI(AsPh_3)_2$, which establishes that $PhPdI(AsPh_3)(DMF)$ is the actual species which reacts with $CH_2{=}CH{-}SnBu_3$ in DMF. A second approach of the reactivity of $PhPdI(AsPh_3)(DMF)$ with $CH_2{=}CH{-}SnBu_3$ is also reported which involves a route initiated through the dimer [$Ph_2Pd_2(\mu^2\text{-}I)_2(AsPh_3)_2$], whose full and fast dissociation in DMF generates $PhPdI(AsPh_3)(DMF)$ prior its reaction with $CH_2{=}CH{-}SnBu_3$.

Results

Kinetics of the Transmetalation Step from $PhPdI(AsPh_3)_2$ in DMF: Principle of the Kinetic Method. Although the complex $PhPdI(AsPh_3)_2$ had been isolated and fully characterized,[8] we preferred to investigate the reactivity of $CH_2{=}CH{-}SnBu_3$ with $PhPdI(AsPh_3)_2$ generated in situ by reacting 1 equiv PhI with $Pd^0(dba)_2$ associated to 2 equivs $AsPh_3$ in DMF (Eq 3,4),[8] to mimic more closely the situation which occurs during a real catalytic cycle.[10]

$$\mathrm{Pd^0(dba)_2 + 2AsPh_3 \longrightarrow Pd^0(dba)(AsPh_3)_2 + dba} \qquad (3)$$

$$\mathrm{Pd^0(dba)(AsPh_3)_2 + PhI \longrightarrow PhPdI(AsPh_3)_2 + dba} \qquad (4)$$

At the initial $Pd^0(dba)_2$ concentration of $C_0 = 2$ mM, the oxidative addition (eq 4) was sufficiently fast ($t_{1/2} = 8$ s at 25 °C) for the transmetalation step to be investigated without any kinetic interference, once the oxidative addition was total.

The reaction of $CH_2{=}CH{-}SnBu_3$ was first monitored by ^1H NMR spectroscopy by reacting two equiv. $CH_2{=}CH{-}SnBu_3$ with $PhPdI(AsPh_3)_2$ in DMF-d_7 at room temperature. This reaction clearly produced styrene in quantitative yield (eq 5).

$$\mathrm{PhPdI(AsPh_3)_2 + CH_2{=}CH\text{-}SnBu_3 \xrightarrow{DMF} Ph\text{-}CH{=}CH_2 + I^- + {}^+SnBu_3 + Pd^0(AsPh_3)_2} \qquad (5)$$

No intermediate complex(es) could be detected in the ^1H NMR spectrum. Moreover, ^1H NMR spectroscopy did not permit to monitor the kinetics of the transmetalation step with sufficient time resolution. Conversely, we observed through conductivity measurements that, in DMF, and over the whole range of millimolar concentrations investigated here, $ISnBu_3$ which is a product of the reaction, was completely dissociated into I^- and $^+SnBu_3$ (eq 5). Because $ISnBu_3$ is generated concomitantly with the coupling product, this observation suggested a facile and very accurate way of monitoring the kinetics of the reaction 5 in DMF with the required time resolution.

(9) Louie and Hartwig have reported that stoichiometric reactions of organostannanes with 16-electron *trans*-$ArPdXL_2$ (L = PPh_3) complexes proceed in toluene via the reaction of 14-electron ArPdXL complexes formed by dissociation of one ligand L (Scheme A).[2] 14-electron diorgano ArPdRL complexes are then formed, which undergo a fast reductive elimination (Scheme A).[2]

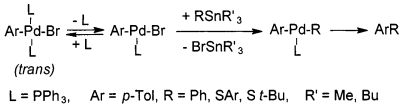

Scheme A. Mechanism of the transmetalation proceeding by prior dissociation of one phosphine ligand L, followed by reductive elimination.[2]

(10) Farina has used $Pd^0{}_2(dba)_3$ as precursor.[3] We used $Pd^0(dba)_2$ because it was used in our previous work[8] to allow a comparison of the reactivity in oxidative addition of Pd^0 ligated to $AsPh_3$ with that of Pd^0 ligated to PPh_3. For a review on $Pd^0(dba)_2$ as precursor, see: Amatore, C.; Jutand, A. *Coord. Chem. Rev.* **1998**, *178*−*180*, 511−528.

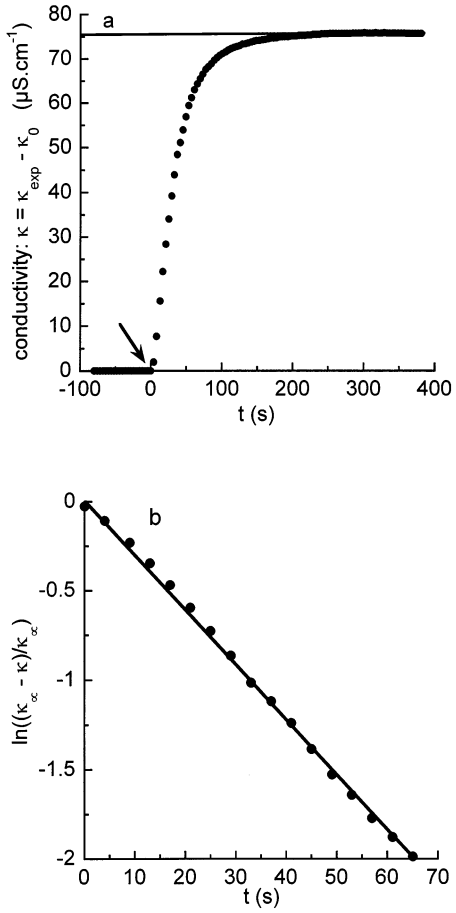

Figure 1. (a) Kinetics of the reaction of $CH_2{=}CH{-}SnBu_3$ (30 mM) with $PhPdI(AsPh_3)_2$ (2 mM) in DMF at 25 °C, as monitored by conductivity measurements of $I^- + {}^+SnBu_3$ (eq 5). $PhPdI(AsPh_3)_2$ was preformed in situ by the reaction of PhI (2 mM) with $Pd^0(dba)_2$ (2 mM) and $AsPh_3$ (4 mM). κ_{exp}: experimental conductivity at *t*, κ_0: residual conductivity (3 $\mu S{\cdot}cm^{-1}$) measured before the addition of $CH_2{=}CH{-}SnBu_3$ (indicated by the arrow) to the preformed $PhPdI(AsPh_3)_2$. (—): conductivity of an authentic sample of $ISnBu_3$ (2 mM) in DMF. (b) Plot of $\ln((\kappa_\infty{-}\kappa)/\kappa_\infty) = \ln x$ versus time (κ: conductivity of $I^- + {}^+SnBu_3$ at *t*, κ_∞: final conductivity). $\ln((\kappa_\infty{-}\kappa)/\kappa_\infty) = -k_{obs}t$.

It was first checked that, in DMF, the conductivity of the solution obtained after reaction of 15 equiv. of $CH_2{=}CH{-}SnBu_3$ with $PhPdI(AsPh_3)_2$ (2 mM) (Figure 1a) resulted identical ($\kappa = 76 \pm 5$ $\mu S.cm^{-1}$ at 25 °C) to that measured for an authentic sample of $ISnBu_3$ (2 mM) in DMF ($\kappa = 75$ $\mu S.cm^{-1}$ at 25 °C). It has also been checked independently that $CH_2{=}CH{-}SnBu_3$ did not exhibit any conductivity in DMF. This ensured that the presence of other reactants and products (eq 5) did not alter the kinetic measurements when monitoring the progress of reaction 5 by conductivity measurements. Therefore, the kinetics of reaction 5, i.e., of the overall transmetalation step could be investigated extremely accurately through the measurement of the rate of formation of $I^- + {}^+SnBu_3$ by conductivity measurements.

In the presence of an excess of $CH_2{=}CH{-}SnBu_3$, the variation of lnx versus time, ($x = (\kappa_\infty{-}\kappa)/\kappa_\infty$); κ: conductivity of $I^- + {}^+SnBu_3$ at t, κ_∞: final conductivity determined in Figure 1a) which characterizes the advancement of the reaction, was linear (Figure 1b). This establishes a reaction order of +1 for the reactive Ph-Pd^{II} complex.[11] The observed rate constant for the formation of $I^- + {}^+SnBu_3$, k_{obs} (s^{-1}) was then determined from the slope of the regression line (Figure 1b), viz., $\ln x = -k_{obs}t$. k_{obs} varied linearly with the $CH_2{=}CH{-}SnBu_3$ concentration (Figure 2), thus establishing a reaction order of +1 in $CH_2{=}CH{-}SnBu_3$.

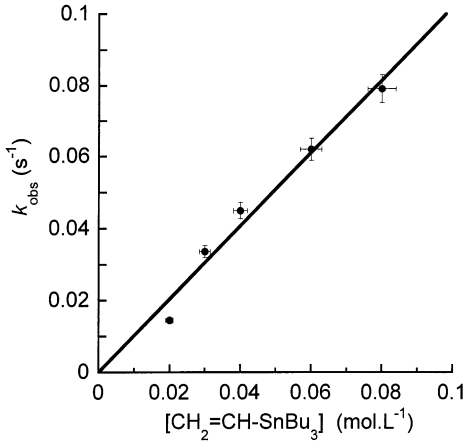

Figure 2. Reaction of $CH_2{=}CH{-}SnBu_3$ with $PhPdI(AsPh_3)_2$ (2 mM) in DMF at 25 °C. Determination of the reaction order in $CH_2{=}CH{-}SnBu_3$: plot of k_{obs}, determined as in Figure 1b, versus $CH_2{=}CH{-}SnBu_3$ concentration. $PhPdI(AsPh_3)_2$ was preformed in situ by the reaction of PhI (2 mM) with $Pd^0(dba)_2$ (2 mM) and $AsPh_3$ (4 mM).

The effect of $AsPh_3$ concentration on the kinetics of the transmetalation step was tested in the range 2−10 mM, by addition of $AsPh_3$ to $PhPdI(AsPh_3)_2$ ($C_0 = 2$ mM) prior to the introduction of $CH_2{=}CH{-}SnBu_3$ (20 mM). $PhPdI(AsPh_3)_2$ was generated in situ by reaction of PhI (2 mM) with $Pd^0(dba)_2$ (2 mM) associated to *n* equiv. $AsPh_3$ ($2 \le n \le 7$). The reaction proceeded slower and slower as the $AsPh_3$ concentration was made larger and larger (Figure 3a) suggesting a decomplexation of one ligand $AsPh_3$ from $PhPdI(AsPh_3)_2$ either before of after reaction with $CH_2{=}CH{-}SnBu_3$.

Kinetics of the Transmetalation Step from $[Ph_2Pd_2(\mu^2\text{-}I)_2(AsPh_3)_2]$ in DMF. Because the dimer $[Ph_2Pd_2(\mu^2\text{-}I)_2(AsPh_3)_2]$ **3** could be considered as a potential source of PhPdI(DMF)(AsPh$_3$) **2** through the equilibrium in eq 6, the dimer **3** was synthesized by reacting PhI with $Pd^0(dba)_2$ and one equiv $AsPh_3$ in THF. THF was chosen as the solvent to facilitate the workup by simple evaporation. Brown yellow crystals were isolated and submitted to X-ray analysis, which revealed the structure of the dimer *trans*-$[Ph_2Pd_2(\mu^2\text{-}I)_2(AsPh_3)_2]$ **3** (eq 7, Figure 4, Table 1).[12]

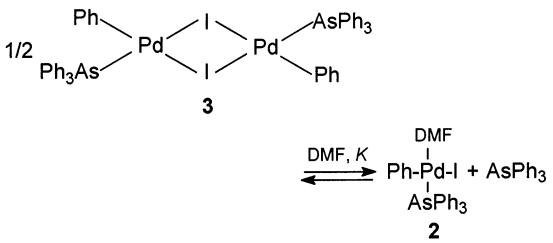

(6)

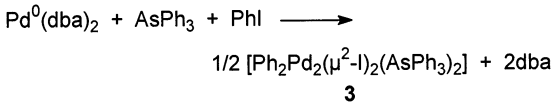

(7)

(11) Some deviation from the linearity was observed (Figure 1b). This is due to a variation of the ligand concentration during the course of the reaction. The exact kinetic law is given in eq 14 in the discussion part with $n = 2$.
(12) For the synthesis of related dimer $[Ph_2Pd_2(\mu^2\text{-}I)_2(PPh_3)_2]$: see: Grushin, V. V.; Alper, H. *Organometallics*, **1993**, *12*, 1890−1901.

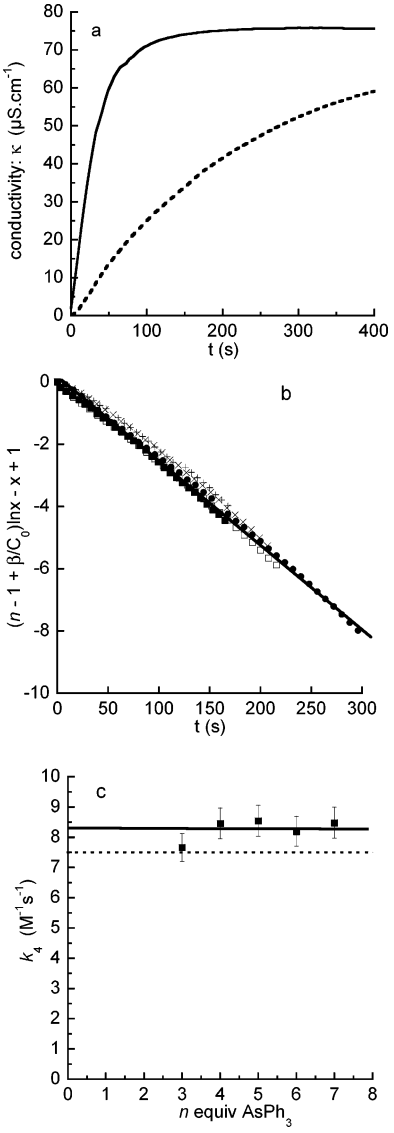

Figure 3. Influence of $AsPh_3$ concentration on the kinetics of the reaction of $CH_2{=}CH{-}SnBu_3$ (20 mM) with $PhPdI(AsPh_3)_2$ (2 mM) in DMF at 25 °C. $PhPdI(AsPh_3)_2$ was preformed in situ by the reaction of PhI (2 mM) with $Pd^0(dba)_2$ (2 mM) and *n* equivs $AsPh_3$. (a) conductivity measured as in Figure 1a, with $n = (-)$ 2; (- - -) 7. (b) Plot of $(n - 1 + \beta/C_0)\ln x - x + 1$ versus time (eq 14) with $n = (+)$ 3; (■) 4; (□) 5; (×) 6; (●) 7 ($x = (\kappa_\infty - \kappa)/\kappa_\infty$; κ: conductivity of $I^- + {}^+SnBu_3$ at *t*; κ_∞: final conductivity). (c) (■) k_4 values calculated from the slope of the straight lines obtained in Figure 3b for each *n* value; (- - -) k_4 value calculated for the reaction of $PhPdI(AsPh_3)$(DMF) (generated from the dimer $[Ph_2Pd_2(\mu_2\text{-}I)_2(AsPh_3)_2]$) with $CH_2{=}CH{-}SnBu_3$ (Figure 5).

To determine whether $CH_2{=}CH{-}SnBu_3$ reacts with $PhPdI(AsPh_3)$(DMF) or with $[Ph_2Pd_2(\mu^2\text{-}I)_2(AsPh_3)_2]$, the kinetics of the reaction of $[Ph_2Pd_2(\mu^2\text{-}I)_2(AsPh_3)_2]$ **3** (1 mM) with 2 equivs $CH_2{=}CH{-}SnBu_3$ in DMF was monitored by the conductivity measurements of $I^- + {}^+SnBu_3$ generated during the reaction, as for $PhPdI(AsPh_3)_2$ (vide supra).[13] Plotting $1/x = \kappa_\infty/(\kappa_\infty - \kappa)$ versus time gave a straight line with an intercept equal to unity (Figure 5) (κ: conductivity of $I^- + {}^+SnBu_3$ at *t*, κ_∞: final conductivity): $1/x = k_{app}t + 1$, attesting a kinetic rate law corresponding to a 1:1 reaction between two reagents present in stoichiometric amounts.

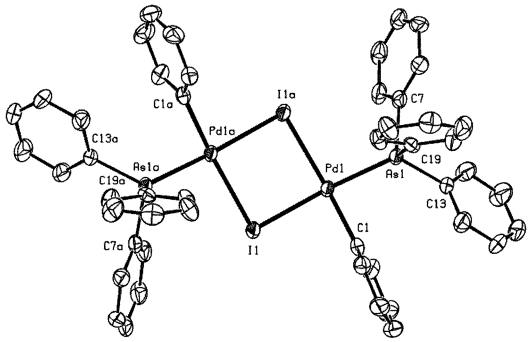

Figure 4. X-ray structure of the dimeric complex $[Ph_2Pd_2(\mu^2\text{-}I)_2(AsPh_3)_2]$ synthesized by reacting PhI with $Pd^0(dba)_2$ and $AsPh_3$ (1 equiv).

Table 1. Crystallographic Data for $[Ph_2Pd_2(\mu^2\text{-}I)_2(AsPh_3)_2]$

molecular formula:	$C_{96}H_{80}As_4I_4Pd_4$
molecular weight:	2466.48
crystal habit:	brownish cube
crystal dimensions (mm):	0.18 × 0.18 × 0.18
crystal system:	monoclinic
space group:	*C*2/*c*
a(Å):	30.404(5)
b(Å):	15.008(5)
c(Å):	19.672(5)
β(°):	102.970(5)
V(Å^3):	8747(4)
Z:	4
d(g-cm^{-3}):	1.873
F000:	4736
μ(cm^{-1}):	3.768
maximum θ:	30.03
HKL ranges:	−42 42; −21 19; −27 27
reflections measured:	22625
independent reflections:	12753
rint:	0.0357
reflections used:	8922
criterion:	> 2sigma(*I*)
refinement type:	Fsqd
hydrogen atoms:	riding
parameters refined:	487
reflections/parameter:	18
wR2:	0.1015
R1:	0.0402
weights a, b1:	0.0486; 0.0000
GoF:	1.014
difference peak/hole (e/Å^3):	2.250(0.152)/−1.417(0.152)

Discussion

Transmetalation Step from $PhPdI(AsPh_3)$(DMF) Generated from $[Ph_2Pd_2(\mu^2\text{-}I)_2(AsPh_3)_2]$ in DMF. From the kinetic law shown in Figure 5: $1/x = k_{app}t + 1$, one deduces that the reaction order in Pd^{II} is clearly not $^1/_2$, which should be the case whenever the dimer **3** would be in rapid equilibrium with its reactive monomeric species **2** $PhPdI(AsPh_3)$(DMF) (eq 6). Indeed, for a reaction of $CH_2{=}CH{-}SnBu_3$ with the monomeric

(13) At the end of the reaction, the final conductivity did not reach the value of $\kappa_\infty = 75\ \mu S{\cdot}cm^{-1}$ expected for a concentration of 2 mM of $I^- + {}^+SnBu_3$, but a lower value of $48\ \mu S{\cdot}cm^{-1}$, although the dimer was totally converted into styrene. We rationalized this lower conductivity by remarking that due to the lack of $AsPh_3$ (only one $AsPh_3$ per palladium is available) the Pd^0 formed in the reaction could be stabilized by complexation of the released iodide ion to afford an ionic complex $Pd^0(AsPh_3)I^-$.[14] The intrinsic conductance of this species is necessarily less than that of the free I^- due to the increased ionic radius. This should account for the observed smaller value of the final conductivity. To test the effect of the complexation of Pd^0 by I^- on the conductivity value, $Pd^0(dba)_2$ (2 mM) was added to a solution of $I^- + {}^+SnBu_3$ (2 mM) in DMF at 25 °C. The initial conductivity of $I^- + {}^+SnBu_3$, $\kappa = 75\ \mu S.cm^{-1}$ dropped to $63\ \mu S{\cdot}cm^{-1}$ when $Pd^0(dba)_2$ was added to the cell, evidencing the complexation of the low ligated Pd^0-(dba) generated in solution in DMF[15] by I^-, to form an anionic complex $Pd^0(dba)I^-$ more bulky than the free I^-.

Scheme 4. Mechanism of the Reaction of $[Ph_2Pd_2(\mu^2\text{-}I)_2(AsPh_3)_2]$ and $CH_2{=}CH{-}SnBu_3$ in DMF

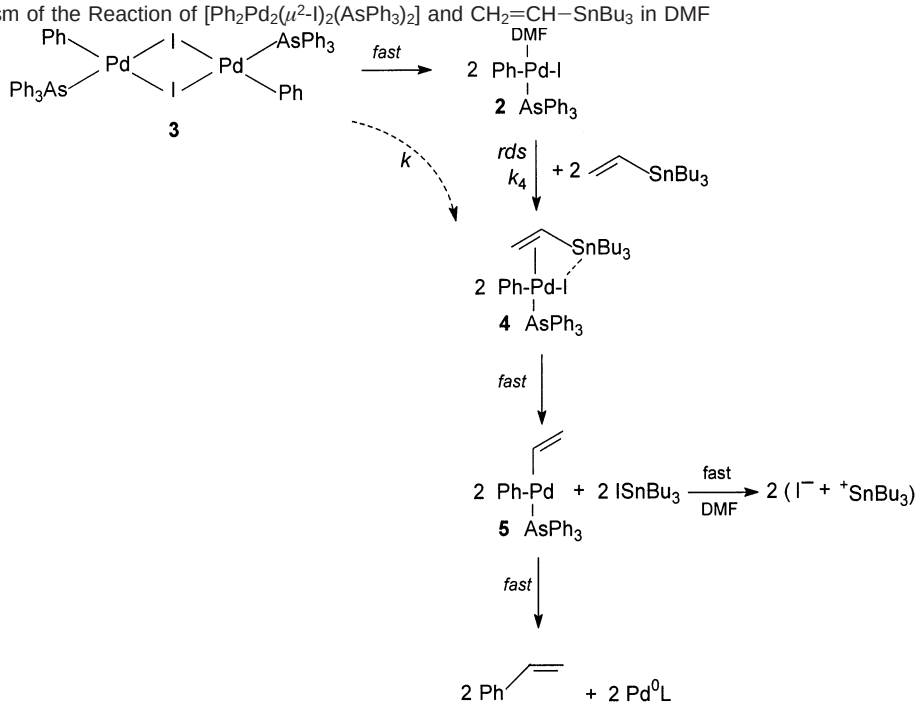

species **2** (rate constant k_4) involved in such an equilibrium with the dimer, the rate law would be: $1/x^{1/2} = k_4KC_0t/2 + 1$. The rate law: $1/x = k_{app}t + 1$ characterizes a rate determining step involving a 1:1 reaction between two reagents present in stoichiometric amounts. Consequently, in DMF the dimer **3** may: (i) dissociate upon dissolution to give $PhPdI(AsPh_3)$-(DMF), which reacts with $CH_2{=}CH{-}SnBu_3$ (rate constant k_4 in Scheme 4) or (ii) be the reactive complex.

Let us first discuss route (ii). At least two mechanisms may be envisaged for the reaction of the dimer **3**. On one hand, a sequential reaction of the dimer with two molecules of $CH_2{=}CH{-}SnBu_3$, the first one giving an equilibrium displaced by the second one to form two molecules of **4** at once. This would lead to a reaction order of 2 for $CH_2{=}CH{-}SnBu_3$. This mechanism is ruled out because the corresponding rate law would be: $1/x^2 = 8kC_0^2t + 1$. On the other hand, a sequential reaction of the dimer **3** with one molecule of $CH_2{=}CH{-}SnBu_3$ reacting irreversibly (rate constant k_1) to form a iodide-monobridged complex in which one Pd^{II} is ligated to $CH_2{=}CH{-}SnBu_3$ as in: $[PhPdL(\eta^2\text{-}CH_2{=}CH{-}SnBu_3)(\mu^2\text{-}I)Pd(Ph)$-$IL]$ **6** (L = $AsPh_3$) and then a fast reaction of the latter species **6** with a second $CH_2{=}CH{-}SnBu_3$ (rate constant k_2) to form two molecules of **4 (**reaction order of 1 for $CH_2{=}CH{-}SnBu_3$ in each step). If $k_2 > k_1$ so that the steady-state approximation may be applied to complex **6**, the rate law is then $1/x = k_1C_0(2 + k_1/k_2)t + 1$. This law is compatible with that found experimentally (vide supra) with $k_{app} = k_1(2 + k_1/k_2)C_0$. If we consider now the route (i) (Scheme 4), the concentration of the monomer **2** is twice that of the dimer, and the rate law is evidently identical to that observed experimentally with $k_{app} = 2k_4C_0$.

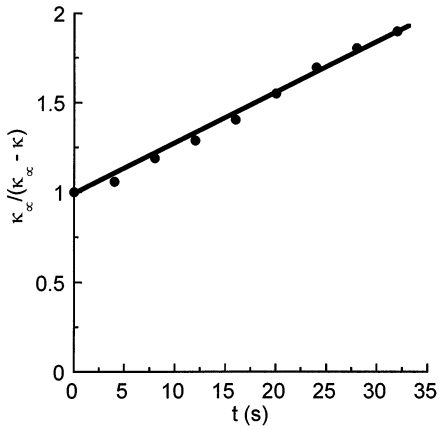

Figure 5. Kinetics of the reaction of $CH_2{=}CH{-}SnBu_3$ (2 mM) with $[Ph_2Pd_2(\mu^2\text{-}I)_2(AsPh_3)_2]$ (1 mM) in DMF at 25 °C, as monitored by conductivity measurements of $I^- + {}^+SnBu_3$ formed in the reaction. Plot of $\kappa_\infty/(\kappa_\infty - \kappa) = 1/x$ versus time (κ: conductivity of $I^- + {}^+SnBu_3$ at t, κ_∞: final conductivity). $1/x = kC_0t + 1$.

On the basis of the kinetic law, it is therefore impossible to discriminate between the dimer **3** or the monomeric complex **2** as the reactive species involved in the reaction with $CH_2{=}CH{-}SnBu_3$.

To solve this conundrum, one needs therefore to assess if upon dissolution in DMF, the dimer dissociates almost irreversibly or not. If it dissociates, then the rate law features the reaction of the monomeric $PhPdI(AsPh_3)_2(DMF)$ with $k_{app} = 2k_4C_0$. If it does not dissociate, the experimental rate law features a sequential attack of the dimer with $k_{app} = k_1(2 + k_1/k_2)C_0$. Spectroscopic investigations were thus performed on solutions of the dimer **3** in DMF, a coordinating solvent as well as in noncoordinating solvents such as $CHCl_3$ and CH_2Cl_2. The UV spectra of the dimer $[Ph_2Pd_2(\mu^2\text{-}I)_2(AsPh_3)_2]$ **3** in $CHCl_3$ or CH_2Cl_2 were similar (Figure 6a). However, in DMF, a different UV spectrum was observed with a shift of the maximum of absorbance of 40 nm to lower wavelengths, indicating that a new species was generated. Moreover, the spectrum in DMF was not concentration dependent. Consequently, in DMF, $[Ph_2Pd_2(\mu^2\text{-}I)_2(AsPh_3)_2]$ is *fully dissociated* to the monomeric species $PhPdI(AsPh_3)(DMF)$ **2** (eq 8).[16,17a] This occurs by a fast reaction irrespective of the fate of **2**. In other words, in chloroform the dimer **3** exists as such whereas in DMF, the

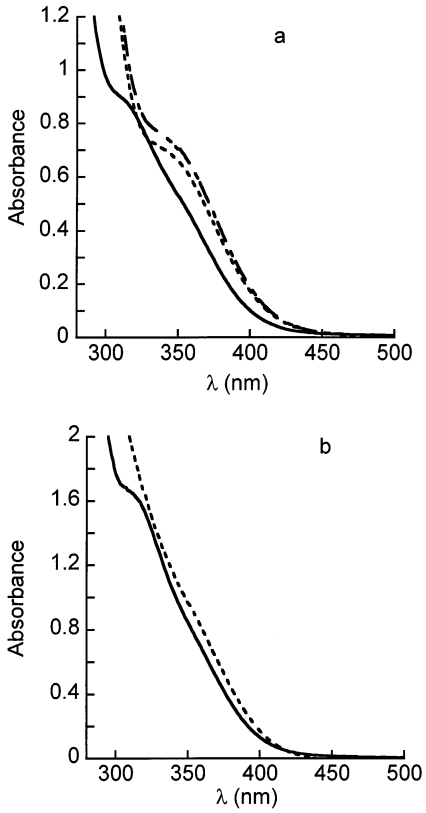

Figure 6. UV spectroscopy in a 1 mm cell at 25 °C: (a) $[Ph_2Pd_2(\mu^2\text{-}I)_2(AsPh_3)_2]$: (— - —) 0.69 mM in CH_2Cl_2; (- - -) 0.64 mM in $CHCl_3$; (—) 0.62 mM in DMF at 25 °C. (b) $PhPdI(AsPh_3)_2$: (- - -) 2.2 mM in $CHCl_3$; (—) 2.2 mM in DMF.

dimer **3** does not exist in appreciable amount. Therefore, in DMF one observes the reactivity of the monomeric complex **2** generated upon its dissociation (eq 8).

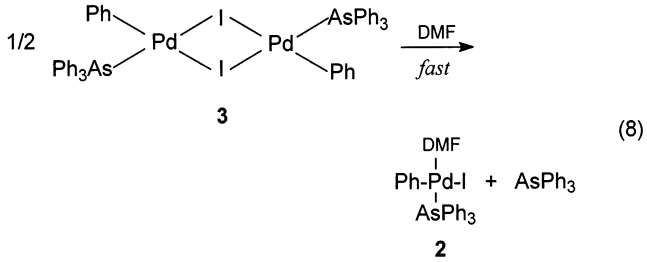

(8)

Consequently, the kinetics observed in Figure 5 characterizes the reactivity of $PhPdI(AsPh_3)(DMF)$ with $CH_2{=}CH{-}SnBu_3$ (Scheme 4). The rate constant $k = 15\ M^{-1}s^{-1}$, calculated from the slope of the straight line ($1/x = kC_0t + 1$) is then: $k = 2k_4$ (Scheme 4). The intrinsic reactivity of $PhPdI(AsPh_3)(DMF)$ with $CH_2{=}CH{-}SnBu_3$ can then be determined by this procedure. This gives: $k_4 = 7.5 \pm 0.5\ M^{-1}s^{-1}$ (DMF, 25 °C).

Transmetalation Step from $PhPdI(AsPh_3)(DMF)$ Generated by Dissociation of $AsPh_3$ from $PhPdI(AsPh_3)_2$ in DMF. Because the dimer $[Ph_2Pd_2(\mu^2\text{-}I)_2(AsPh_3)_2]$ does not exist in solution in DMF (eq 8), the only equilibrium operating in DMF when starting from $PhPdI(AsPh_3)_2$ involves $PhPdI(AsPh_3)(DMF)$ (eq 9), as written in our previous paper (Scheme 3).[8]

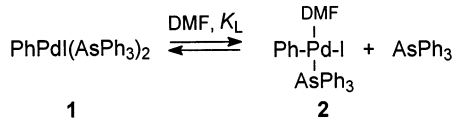

(9)

This has been confirmed by the UV spectrum of $PhPdI(AsPPh_3)_2$ in DMF (Figure 6b) which exhibited the same absorption band at 310 nm as that observed in Figure 6a in DMF, characteristic of $PhPdI(AsPh_3)(DMF)$ generated from the dimer **3** (eq 8).[17b] Consequently, in DMF, under these conditions only two species are prone to react with $CH_2{=}CH{-}SnBu_3$: $PhPdI(AsPh_3)(DMF)$ or $PhPdI(AsPPh_3)_2$.

According to Farina[3a] and Espinet,[4b] although their results apply to THF, we need to consider two limiting mechanisms for the transmetalation step: (i) reaction of $CH_2{=}CH{-}SnBu_3$ with $PhPdI(AsPh_3)_2$ **1**[4b] via a pentacoordinated Pd^{II} transition state $[PhPdIL_2(\eta^2\text{-}CH_2{=}CH{-}SnBu_3)]^{\ddagger}$[4b] (Scheme 5, route A in which however complex **2** must be taken into account because of the partial dissociation of complex **1** in eq 9 before reaction of **1** with $CH_2{=}CH{-}SnBu_3$) or (ii) reaction of $CH_2{=}CH{-}SnBu_3$ with $PhPdI(AsPh_3)(DMF)$ **2** formed from **1** by the prior decomplexation of one ligand $AsPh_3$[3a] (Scheme 5, route B).[19]

Because no intermediate complex(es) could be detected by ^1H NMR spectroscopy during the course of the reaction up to the styrene formation (vide supra), neither the intermediate complex **4** nor **5** could accumulate in significant amount (Scheme 5). Therefore, their concentration represents at most a few percent of the palladium concentration and they behave as transient species obeying steady-state kinetics. This establishes

(14) It is well established that low ligated Pd^0 complexes are stabilized by halide ions to form anionic species $Pd^0L_2X^-$ (X = Cl, Br, I.; L = PPh_3) with the order of stabilization: $I^- > Br^- > Cl^-$. See: Amatore, C.; Azzabi, M.; Jutand, A. *J. Am. Chem. Soc.* **1991**, *113*, 8375−8384.

(15) Amatore, C.; Jutand, A.; Khalil, F.; M'Barki, M. A.; Mottier, L. *Organometallics* **1993**, *12*, 3168−3178.

(16) Lo Sterzo et al. have reported the irreversible dissociation of a related dimer into the corresponding monomer in DMF (as evidenced by the shift of 30 nm of the absorption band toward lower wavelengths explained by the conversion of the dimer to the monomer upon switching from CH_2Cl_2 to DMF).[6]

(17) (a) The ^1H NMR spectrum of $PhPdI(AsPh_3)(DMF)$ complex generated from the dimer $[Ph_2Pd_2(\mu^2\text{-}I)_2(AsPh_3)_2]$ (eq 8) exhibited two broad signals (Figure 7a and Experimental Section), which are assigned to the protons of the Ph linked to the Pd^{II} in $PhPdI(AsPh_3)(DMF)$. In that case the *p*-H and *m*-H could not be distinguished and no coupling detected. This may be due to a fast exchange of the DMF ligand or to a fast isomerization of $PhPdI(AsPh_3)(DMF)$ complexes as suggested in eq A.

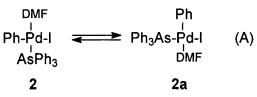

The complex in which the ligands Ph and $AsPh_3$ would be in a trans position on the Pd^{II} center is less probable because of the *transphobia*[18] of Ph and $AsPh_3$ ligands. The reaction of both complexes **2** and **2a** with $CH_2{=}CH{-}SnBu_3$ will generate complexes of type **4**, in which the ligands $CH_2{=}CH{-}SnBu_3$ and iodide are in a cis position in favor of an easy elimination of $ISnBu_3$. (b) The ^1H NMR signals of $PhPdI(AsPh_3)_2$[8] in the absence of excess $AsPh_3$ were not well resolved in DMF (Figure 7b, and the Experimental Section). A broad signal was observed for the *o*-H and a unique broad signal for the *m*-H and *p*-H of the Ph group linked to the Pd^{II} attesting the existence of an equilibrium involving $PhPdI(AsPh_3)_2$. Upon addition of 6 equivs $AsPh_3$ to $PhPdI(AsPh_3)_2$ in DMF-d_7, a well resolved spectrum was observed for $PhPdI(AsPh_3)_2$ similar to that observed in Figure 7c, showing that the equilibrium relating $PhPdI(AsPh_3)_2$ to $PhPdI(AsPh_3)(DMF)$ and $AsPh_3$ (eq 9) was then completely shifted towards $PhPdI(AsPh_3)_2$. As expected for the equilibrium in eq 9, the protons of the Ph group linked to the Pd^{II} in $PhPdI(AsPh_3)_2$ in the absence of $AsPh_3$ (Figure 7b) are located between those of $PhPdI(AsPh_3)(DMF)$ (Figure 7a)[17a] and those of $PhPdI(AsPh_3)_2$ observed in the presence of excess $AsPh_3$ (Figure 7c).

(18) Vivente, J.; Arcas, A.; Bautista, D.; Jones, P. G. *Organometallics* **1997**, *16*, 2127−2138.

(19) Very recently, Lo Sterzo et al.[6] established that the transmetalation of $PhC{\equiv}C{-}SnBu_3$ in a Stille-type reaction in DMF may occur by the two mechanisms postulated by Farina[3a] and Espinet,[4b] that is involving the prior dissociation of the ligand L (L = PPh_3) or not. In the latter case, the related pentacoordinated Pd^{II} complex postulated as a transition state by Casado and Espinet[4b] has been characterized and demonstrated to be a true reaction intermediate.[6]

Scheme 5. Possible Mechanisms for the Formation of Styrene from $PhPdI(AsPh_3)_2$ and $CH_2{=}CH{-}SnBu_3$ in DMF: Reaction of $CH_2{=}CH{-}SnBu_3$ with Either $PhPdI(AsPh_3)_2$ **1** (route A)[4b] or with $PhPdI(AsPh_3)(DMF)$ **2** (route B)[3] Formed by Dissociation of One Ligand $AsPh_3$ from **1**

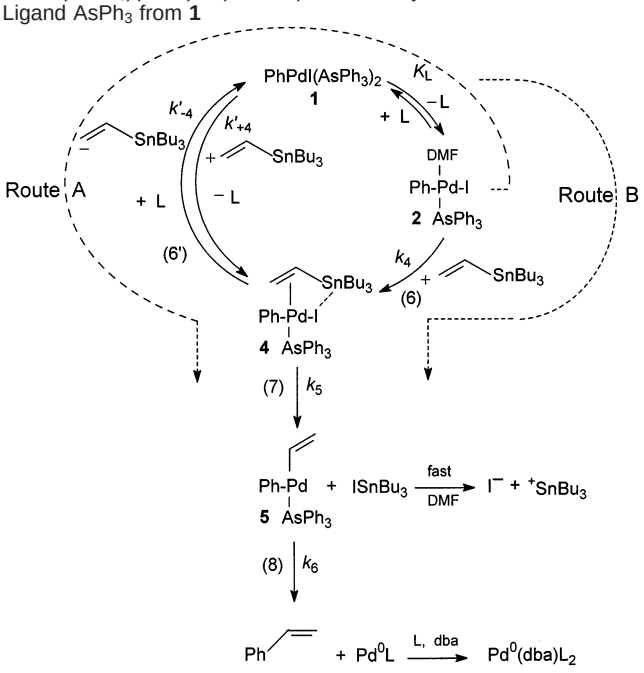

that the rate of appearance of the $I^- + {}^+SnBu_3$ species is identical to that of the generation of complexes **4** and **5**. In other words, the conductivity measurements reflect exactly the kinetics of the transmetalation step. The fact that the rate of formation of $I^- + {}^+SnBu_3$ obeys a first-order reaction in $CH_2{=}CH{-}SnBu_3$ also confirms the hypothesis made just above, i.e., that reaction 7 in Scheme 5 is much faster than the formation of the intermediate complex **4**.

The kinetic law for the mechanism A (Scheme 5) is given by eq 10, upon considering steady-state approximation for complex **4** and taking into account the partial dissociation of $PhPdI(AsPPh_3)_2$ to $PhPdI(AsPPh_3)(DMF)$ in eq 9 (L: $AsPh_3$; Sn: $CH_2{=}CH{-}SnBu_3$).[20]

$$d[I^-]/dt = d[{}^+SnBu_3]/dt = -\,d[\mathbf{1}]/dt = \frac{k'_{+4}k_5[\mathbf{1}][Sn]([L] + K_L)}{(k'_{-4}[L] + k_5)[L]} \qquad (10)$$

The factor $([L] + K_L)/[L]$ represents the contribution of the partial dissociation of $PhPdI(AsPPh_3)_2$ to $PhPdI(AsPPh_3)(DMF)$ (eq 9), where $K_L = 3.1 \times 10^{-4}$ M in DMF (25 °C).[8]

The kinetic law for the mechanism B (Scheme 5) is given by eq 11. Complex **2** cannot obey a steady state because we observed previously that the $AsPh_3$ dissociation occurred up to ca. 32% in DMF ($K_L = 3.1 \times 10^{-4}$ mol L^{-1}).[8] The mechanism B proceeds then through a Michaelis−Menton type kinetics[20c] with the rate law given in eq 11.[4b,20c]

$$d[I^-]/dt = d[{}^+SnBu_3]/dt = -\,d[\mathbf{1}]/dt = \frac{k_4K_L[\mathbf{1}][Sn]}{[L] + K_L} \qquad (11)$$

The kinetics of the transmetalation step has been investigated for added $AsPh_3$ in the range 2−10 mM. In our series of experiments, K_L/L then varied from 0.15 to 0.03. Consequently, eq 10 may simplify to eq 12 ($K'_4 = k'_{+4}/k'_{-4}$) at high L concentration viz. for [L] > 6 mM.

$$-\,d[\mathbf{1}]/dt = \frac{k'_{+4}k_5[\mathbf{1}][Sn]}{k'_{-4}[L] + k_5} = \frac{k_5K'_4[\mathbf{1}][Sn]}{[L] + k_5/k'_{-4}} \qquad (12)$$

Noteworthy, eq 11 (always true) and 12 (valid for [L] > 6 mM) have the same mathematical structure, so that routes A and B could not be distinguished in the basis of the observed rate law at high L concentrations. Both laws can be expressed as in eq 13 with $\alpha = k_4K_L$ and $\beta = K_L$ for eq 11 and $\alpha = k_5K'_4$ and $\beta = k_5/k'_{-4}$ for eq 12.

$$-\,d[\mathbf{1}]/dt = \frac{\alpha[\mathbf{1}][Sn]}{[L] + \beta} \qquad (13)$$

Due to the limiting solubility of $AsPh_3$ in DMF (14 mM), $AsPh_3$ could not be added in larger excess. Therefore, the $AsPh_3$ concentration could not be considered as being constant during the reaction. Taking that into account, integration of eq 13 afforded eq 14 with $x = (\kappa_\infty - \kappa)/\kappa_\infty$ and n being the initial equiv of $AsPh_3$ added to $Pd^0(dba)_2$ before the generation of $PhPdI(AsPh_3)_2$.

$$(n - 1 + \beta/C_0)\ln x - x + 1 = -\,\frac{\alpha[Sn]\,t}{C_0} \qquad (14)$$

A value of $\beta = 3.2 \times 10^{-4}$ was determined so that all unified plot of $(n - 1 + \beta/C_0)\ln x - x + 1$ versus time was linear irrespective n (Figure 3b). These experimental kinetics thus agree with eq 14. Furthermore, treating each series of experiments corresponding to a single n value established also the validity of eq 14, and afforded identical values for the individual slopes (Figure 3b). Consequently, the experimental kinetics of the transmetalation step is in agreement with the framework of the mechanism B (Scheme 5) since eq 14 was shown to be valid all over the range of $AsPh_3$ concentration added to $PhPdI(AsPh_3)_2$ (2−10 mM). This would not be the case for the mechanism A because eq 12 is valid only for high $AsPh_3$ concentrations (>6 mM). Therefore, these kinetic results disprove the mechanism A and sustain mechanism B. Consequently, $\beta = 3.2 \pm 0.1 \times 10^{-4}$ M (DMF, 25 °C) affords a second determination of K_L in agreement with the value of $K_L = 3.1 \times 10^{-4}$ M (DMF, 25 °C) determined in our previous work,[8] because $\beta = K_L$ for mechanism B (see above).

An average value of α can be calculated from the average slope of the straight lines of Figure 3b or by averaging the slopes obtained for each n values. Because $\alpha = k_4K_L$, then $k_4 = 8.3 \pm 0.5$ $M^{-1}s^{-1}$. This value of k_4 is extremely close to that determined from the kinetics of the transmetalation step ($k_4 = 7.5$ $M^{-1}s^{-1}$), investigated upon starting from $PhPdI(AsPh_3)(DMF)$ generated by the fast dissociation of the dimer **3** (vide supra and Figure 3c). Moreover, it is compatible with that reported by Farina ($k_4 = 108$ $M^{-1}s^{-1}$ in THF at 50 °C) considering the change of solvent and temperature.[3]

At this stage, we have thus shown experimentally that the mechanism B in Scheme 5 is coherent with the kinetics of the transmetalation step, whereas that in mechanism A is not coherent except at large [L] values. The corresponding rate law (eq 11, 14) is obeyed and the values of the coefficient K_L and

(20) (a) Gellene, G. I. *J. Chem. Educ.* **1995**, *72*, 196−199. (b) Andraos, J. *J. Chem. Educ.* **1999**, *76*, 1578−1583. (c) Jencks W. P. *Catalysis in Chemistry and Enzymology*; Dover, Ed., John Wiley & Sons: 1987; p 571.

k_4 determined on the basis of this rate law are fully coherent with the values of K_L and k_4 determined independently by two different strategies applied to different series of experiments, since PhPdI($AsPh_3$)(DMF) could be generated in DMF either from the dimer [$Ph_2Pd_2(\mu^2\text{-}I)_2(AsPh_3)_2$] (eq 8) or from PhPdI-($AsPh_3$)$_2$ (eq 9).[8]

The same value of K_L was determined: (i) from the observation of the partial dissociation of PhPdI($AsPh_3$)$_2$ to PhPdI($AsPh_3$)(DMF) in DMF (eq 9, previous work)[8] and (ii) from the kinetics of the transmetalation step performed from PhPdI($AsPh_3$)$_2$ (this work). Similarly the same value of k_4, which characterizes the reactivity of PhPdI($AsPh_3$)(DMF) with CH_2=CH−$SnBu_3$, has been determined (i) from the kinetics of the reaction of CH_2=CH−$SnBu_3$ with PhPdI($AsPh_3$)(DMF) generated by the fast dissociation of the dimer **3** in DMF (this work) and (ii) from the kinetics of the transmetalation step performed from PhPdI($AsPh_3$)$_2$ (this work). This definitively proves that, mechanism B alone is able to sustain kinetically a rate equal to the one determined experimentally in DMF. This evidences that whenever mechanism A occurs in DMF, it may only accounts for a minor contribution in parallel with the major route B. Such a minor contribution may actually exist and be the explanation why k_4, as determined from PhPdI($AsPh_3$)$_2$, viz. $k_4 = 8.3$ $M^{-1}s^{-1}$, is slightly larger (10%) than k_4, as determined from the dimer route, viz. $k_4 = 7.5$ $M^{-1}s^{-1}$. However, this participation may account at maximum for 10% of the reaction.[21]

Transmetalation from *trans*-PhPdI(PPh_3)$_2$ in DMF. The reactivity of CH_2=CH−$SnBu_3$ (50 equiv) with *trans*-PhPdI-(PPh_3)$_2$ generated in situ by the oxidative addition of PhI (1 equiv) with $Pd^0(dba)_2$ and PPh_3 (2 equiv)[15] in DMF has also been monitored through the conductivity measurements of I^- + $^+SnBu_3$ because those species are formed in the cross-coupling reaction (eq 15).

$$PhPdI(PPh_3)_2 + CH_2\text{=}CH\text{-}SnBu_3 \xrightarrow{DMF} Ph\text{-}CH\text{=}CH_2 + I^- + {}^+SnBu_3 + Pd^0(PPh_3)_2 \quad (15)$$

The reaction was found to be 670 times slower than that with PhPdI($AsPh_3$)$_2$ at 25 °C. This confirms that the higher efficiency of $AsPh_3$ compared to that of PPh_3 in the catalytic reaction in DMF is due to the faster transmetalation step as initially proposed by Farina in THF.[3,22]

Equilibrium between [$Ar_2Pd_2(\mu^2\text{-}I)_2(AsPh_3)_2$] and ArPdI-($PPh_3$)$_2$ in Chloroform. The dimer [$Ph_2Pd_2(\mu^2\text{-}I)_2(AsPh_3)_2$] **3** exhibited in $CDCl_3$ the same well resolved ^{1}H NMR spectrum (see the Experimental Section) as that of the complex generated from PhPdI($AsPh_3$)$_2$ after dissociation of one $AsPh_3$ (Figure 5a in our previous paper)[8] which was assigned to PhPdI($AsPh_3$)-*S*.[8] However, one referee of this work drawn our attention to a work (still unpublished at that time) which reported that in $CDCl_3$, the species involving only one $AsPh_3$ per Pd^{II} center could not be PhPdI($AsPh_3$)*S*, due to the poor coordination properties of chloroform, but the dimer **3** (eq 16).[23] We therefore checked (Figure 6a) that the dimer **3** exhibited the same UV spectrum in $CHCl_3$ and in CH_2Cl_2, which is an even less coordinating solvent. The spectrum in DMF was different (vide supra, Figure 6a) due to the irreversible formation of PhPdI-($AsPh_3$)(DMF). Consequently, the dimer **3** most presumably does not dissociate in chloroform. So that the complex formed by the partial dissociation of PhPdI($AsPh_3$)$_2$ in chloroform that we observed by ^{1}H NMR[8] is most certainly the dimer **3** (Eq 16).

$$PhPdI(AsPh_3)_2 \underset{\textbf{2}}{\rightleftharpoons} 1/2\ \textbf{3} + AsPh_3 \quad (16)$$

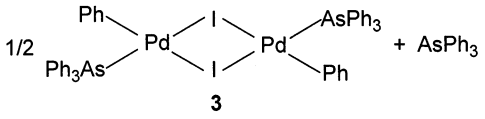

This was confirmed by the UV spectrum of PhPdI($AsPPh_3$)$_2$ in chloroform (Figure 6b), which exhibited the same absorption band at 350 nm as that of the dimer in chloroform (Figure 6a). The equilibrium (16) is slow compared to the time scale of the NMR, since thin well resolved signals were observed for the protons of the Ph attached to the Pd^{II} centers in both complexes **2** and **3** (Figure 5a in our previous paper).[8]

On the basis of the spectroscopic data reported in this paper, it appears that in chloroform PhPdI($AsPh_3$)$_2$ dissociates to form the dimer **3** (eq 16),[24] whereas in DMF, it gives gives PhPdI-($AsPh_3$)(DMF) (eq 9). Whatever the structure of the complex in which the Ph−Pd^{II} is ligated by only one $AsPh_3$, i.e., monomer in DMF or dimer in chloroform, this evidences that *PhPdI*($AsPh_3$)$_2$ *easily releases one ligand* $AsPh_3$ *in appreciable amount in both solvents.*

The dissociation of one $AsPh_3$ in chloroform has also been observed for (*p*-Z−C_6H_4)PdI($AsPh_3$)$_2$ complexes (Z = Cl, OMe), formed in situ by the oxidative addition of *p*-Z−C_6H_4–I to $Pd^0(dba)_2$ and 2 equivs $AsPh_3$ in $CDCl_3$ (eq 17) and characterized by ^{1}H NMR spectroscopy (experimental part).

$$Pd^0(dba)_2 + 2AsPh_3 + p\text{-}Z\text{-}C_6H_4\text{-}I \longrightarrow (p\text{-}Z\text{-}C_6H_4)PdI(AsPh_3)_2 + 2dba \quad (17)$$

$$(p\text{-}Z\text{-}C_6H_4)PdI(AsPh_3)_2 \rightleftharpoons 1/2\ [(p\text{-}Z\text{-}C_6H_4)_2Pd_2(\mu^2\text{-}I)_2(AsPh_3)_2] + AsPh_3 \quad (18)$$

Besides the two major thin doublets of the aromatic protons of *p*-Z−C_6H_4 of the saturated complex (*p*-Z−C_6H_4)PdI($AsPh_3$)$_2$, two minor thin doublets were detected and assigned to the aromatic protons of *p*-Z−C_6H_4 in the dimer [(*p*-Z−C_6H_4)$_2$$Pd_2I_2$-($AsPh_3$)$_2$] (eq 18). They disappeared when $AsPh_3$ was added into the NMR tube. Only the two doublets of complexes (*p*-

(21) This ratio (10%) has to be considered as the maximum relative participation of mechanism A. Indeed, one may consider alternatively that the measurements involving the dimer afforded a slightly lower value of k_4 than the true one, whenever the dimer dissociation was not irreversible enough to afford instantly a concentration exactly double for the reactive monomer. Thus, $k = 2(1 - \epsilon)k_4$, where ϵ may not be exactly zero at initial time. This would not be apparent in a plot such as that in Figure 5, provided ϵ was small ($\leq$10%) but may affect correspondingly the k_4 value determined from the measured k value.

(22) (a) To the best of our knowledge, the dissociation of one PPh_3 from PhPdI-(PPh_3)$_2$ has never been observed in chloroform, nor in DMF. However, in DMF the partial ionization of PhPdI(PPh_3)$_2$ to *trans*-PhPd(PPh_3)$_2$(DMF)$^+$ and I^- has been observed.[22b] A conductivity of 10 μS was measured for the solution of PhPdI(PPh_3)$_2$ (2 mM) in DMF, before the addition of CH_2=CH−$SnBu_3$. Consequently, a reaction of CH_2=CH−$SnBu_3$ with the cationic complex *trans*-PhPd(PPh_3)$_2$(DMF)$^+$ is not excluded, leading to an intermediate *trans*-PdPd(η^2-CH_2=CH−$SnBu_3$)(PPh_3)$_2^+$ complex. (b) Amatore, C.; Carré, E., Jutand, A. *Acta Chem. Scand.* **1998**, *52*, 100−106.

(23) This suggestion was further clarified through a personal communication with Prof. P. Espinet (Poster at the ISCH 13 Meeting in Tarragona, Spain. 3−7 September 2002). Casares, J. A.; Espinet, P.; Salas, G. *Chem. Eur. J.* **2002**, *8*, 4844−4853.

Scheme 6. Mechanism of the Stille Reaction in DMF: Cross-coupling of PhI with $CH_2{=}CH{-}SnBu_3$ Catalyzed by $Pd^0(dba)_2$ Associated to $AsPh_3$ (2 equiv.) (the steps indicated by the dashed arrows are too fast for their kinetics to be monitored here)

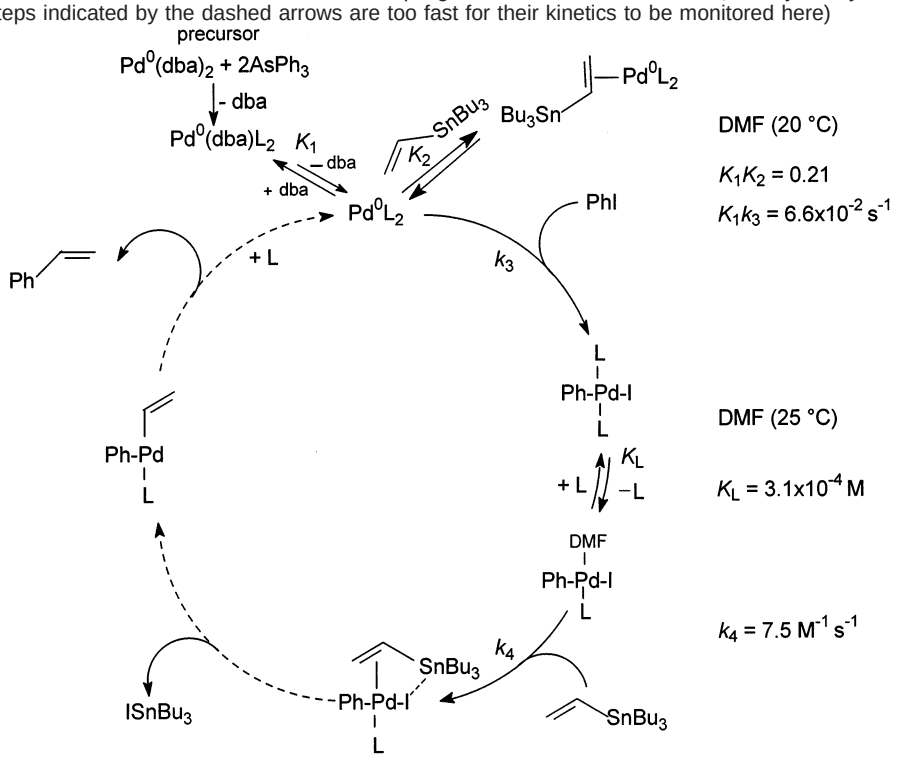

$Z{-}C_6H_4)PdI(AsPh_3)_2$ were then detected in agreement with the shift of the equilibrium in Eq 18 toward its left-hand side. The $AsPh_3$ dissociation percentage did not depend significantly on the substituent Z investigated here (16% for Z = OMe and 18% for Z = Cl). This is consistent with the fact that the aryl ligand cannot exert any trans effect on the dissociation of the $AsPh_3$ ligand due to the trans structure of $(p\text{-}Z{-}C_6H_4)PdI(AsPh_3)_2$.

(24) The reactivity of the dimer $[Ph_2Pd_2(\mu^2\text{-}I)_2(AsPh_3)_2]$ has been investigated in chloroform. Its reaction with 4 equivs $CH_2{=}CH{-}SnBu_3$ was first monitored by ^1H NMR in $CDCl_3$ at room temperature. Styrene was formed in a fast reaction, which thus excluded the possibility to detect any intermediate complex(es). $[Ph_2Pd_2(\mu^2\text{-}I)_2(AsPh_3)_2]$ was totally converted in that reaction. The kinetics of the reaction of $[Ph_2Pd_2(\mu^2\text{-}I)_2(AsPh_3)_2]$ (0.5 mM) with $CH_2{=}CH{-}SnBu_3$ (1 mM) in chloroform was then monitored by UV spectroscopy at 290 nm. The plot of $1/x$ versus time was linear: $1/x = k_{app}t + 1$ ($x = (D - D_\infty)/(D_0 - D_\infty)$; D_0: initial absorbance, D_∞: final absorbance, D: absorbance at t) with $k_{app} = 0.005\ s^{-1}$ at 25 °C. This confirms that in chloroform, the dimer is not involved in an uphill equilibrium with a monomer (equilibrium constant K) which would be the reactive intermediate. Indeed, the rate law would then be: $1/x^{1/2} = k_4KC_0t/2 + 1$ (vide supra). Consequently, the dimer **3** reacts directly with $CH_2{=}CH{-}SnBu_3$ in chloroform. Again two mechanisms are possible as discussed above for the reaction in DMF. The mechanism compatible with the kinetic law is the one in which the dimer reacts first with one molecule of $CH_2{=}CH{-}SnBu_3$ to form the transient complex $[PhPdL(\eta^2\text{-}CH_2{=}CH{-}SnBu_3)(\mu^2\text{-}I)Pd(Ph)IL]$ **6** (irreversible reaction with a rate constant k_1), which then reacts with a second molecule of $CH_2{=}CH{-}SnBu_3$ (rate constant k_2) to form two molecules of complex **4**. The rate law is then $1/x = k_1C_0(2 + k_1/k_2)t + 1$ with $k_{app} = k_1(2 + k_1/k_2)C_0$. Then $k_1(2 + k_1/k_2) = 10\ M^{-1}s^{-1}$. If $k_2 \gg k_1$, as it is most presumable, then $k_1 = 5\ M^{-1}s^{-1}$ ($CHCl_3$, 25 °C). This establishes that the dimer $[Ph_2Pd_2(\mu^2\text{-}I)_2(AsPh_3)_2]$ is the reactive species in chloroform whereas $PdPdI(AsPPh_3)(DMF)$ is the reactive species in DMF (vide supra). It is noteworthy that the value of the rate constant k_1 is close to that ($k_4 = 7.5\ M^{-1}s^{-1}$) determined for $PhPdI(AsPh_3)(DMF)$ in DMF. The followed route does not really stem from the intrinsic reactivity of each species but rather from their relative concentration, which is imposed in each solvent by the ability of the dimer to dissociate or not. The reaction of $PhPdI(AsPh_3)_2$ with $CH_2{=}CH{-}SnBu_3$ was monitored by ^1H NMR spectroscopy in $CDCl_3$. This reaction produced styrene in quantitative yield. Because we have shown in this work that $PhPdI(AsPh_3)_2$ is involved in an equilibrium with $[Ph_2Pd_2(\mu^2\text{-}I)_2(AsPh_3)_2]$ (eq 18), it could have been of interest to determine whether $CH_2{=}CH{-}SnBu_3$ reacts with $PhPdI(AsPh_3)_2$ or with $[Ph_2Pd_2(\mu^2\text{-}I)_2(AsPh_3)_2]$ in chloroform. However, because Stille reactions are never performed in chloroform, this investigation has not been undertaken.

Conclusion

In DMF, at 25 °C, the transmetalation step of the Stille reaction involving $CH_2{=}CH{-}SnBu_3$ as the nucleophile has been found to proceed mainly via the 1:1 reaction of the tin derivative with $PhPdI(AsPh_3)(DMF)$ formed by the dissociation of one ligand $AsPh_3$ from $PhPdI(AsPh_3)_2$. This is in agreement with Farina's conclusions for the same reactants and ligand, despite the change of experimental conditions (THF, 50 °C). The complex $PhPdI(AsPh_3)(DMF)$ is therefore the reactive species which affords styrene following its reaction with the nucleophile $CH_2{=}CH{-}SnBu_3$. The same complex $PhPdI(AsPh_3)(DMF)$ is also generated in DMF from the dimeric complex $[Ph_2Pd_2(\mu^2\text{-}I)_2(AsPh_3)_2]$, which has been independently synthesized and characterized by its X-ray structure. The intrinsic reactivity of $PhPdI(AsPh_3)(DMF)$ with $CH_2{=}CH{-}SnBu_3$ in DMF has been characterized through two different kinetic routes and led to the determination of the same rate constant $k_4 = 7.5\ M^{-1}s^{-1}$ (Scheme 6).

We established in a previous work that the role of $AsPh_3$, compared to PPh_3, is to accelerate the oxidative addition by a 10-fold factor in DMF.[8] However, this effect is partly canceled out in the presence of the nucleophile $CH_2{=}CH{-}SnBu_3$, which interferes in the catalytic cycle prior to the oxidative addition. This results in a decelerating effect due to the partial complexation of the reactive complex $Pd^0(AsPh_3)_2$ by $CH_2{=}CH{-}SnBu_3$ to form the unreactive $Pd^0(\eta^2\text{-}CH_2{=}CH{-}SnBu_3)(AsPh_3)_2$.[8,25] Consequently, in DMF at least the mechanism of the catalytic Stille reaction is much more complex than classically reported (Schemes 1 and 2). This is examplified in Scheme 6, where the rate constants K_1k_3,[8] k_4 and the equilibrium constants K_1K_2,[8] and K_L,[8] for the ligand dissociation, have been determined in DMF.

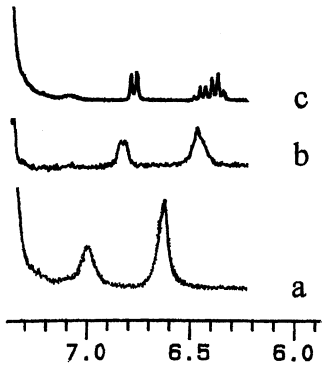

Figure 7. ^{1}H NMR (250 MHz, DMF-d_7, ppm vs TMS): (a) PhPdI(AsPh$_3$)(DMF) from [Ph$_2$Pd$_2$(μ^2-I)$_2$(AsPh$_3$)$_2$] (3 mM); (b) PhPdI(AsPh$_3$)$_2$[8] (4 mM); (c) [Ph$_2$Pd$_2$(μ^2-I)$_2$(AsPh$_3$)$_2$] (3 mM) and AsPh$_3$ (5 equivs). The spectrum observed upon addition of AsPh$_3$ (6 equivs) to PhPdI(AsPh$_3$)$_2$[8] (3 mM), is identical to that in (c).

As established in this work, the greater efficiency of the Stille reaction, when catalyzed by a Pd^0 complex ligated by AsPh$_3$ instead of PPh$_3$, is thus due to an easier dissociation of AsPh$_3$ from PhPdI(AsPh$_3$)$_2$ in THF and DMF. Therefore, besides establishing the central involvement of PhPdI(AsPh$_3$)(DMF) in the Stille reaction in DMF, thereby confirming Farina's proposal in THF, this work demonstrates the essential kinetic role of such species on the efficiency of Stille reactions performed with AsPh$_3$ ligated palladium catalysts. It is noteworthy that within the range of AsPh$_3$ concentrations investigated here, even if PhPdI(AsPh$_3$)(DMF) is no longer detected in the ^{1}H NMR spectrum in the presence of the highest excess of AsPh$_3$ (Figure 7c), it remains the reactive complex, which is then present at a lower concentration and is at the origin of the slower transmetalation step.[26]

However, when considering aryl iodides, which are highly substituted by electron-withdrawing groups such as in C$_6$Cl$_2$F$_3$-I, Espinet et al. have established that ArPdI(AsPh$_3$)$_2$ complexes are the reactive species in THF.[4b] This shows that the structure of the reactive complex (ligated by one or two L ligands) is highly dependent on the aryl group.

Experimental Section

All experiments were performed under a dry atmosphere of Argon by following conventional Schlenk techniques. ^{1}H NMR spectra were recorded on a Bruker spectrometer (250 or 400 MHz). Conductivity was measured on a Radiometer Analytical CDM210 conductivity meter (cell constant = 1 cm^{-1}). Crystallographic data for [Ph$_2$Pd$_2$(μ_2−I)$_2$(AsPh$_3$)$_2$] were collected on a KappaCCD diffractometer at 150.0(1)K with graphite monochromated MoKα radiation (λ = 0.71073 Å). Crystallographic results are summarized in Table 1. Full details of the crystallographic analysis are described in the Supporting Information.

Materials. Dimethylformamide was distilled from calcium hydride under vacuum. Tetrahydrofuran was distilled from sodium-benzophenone. Triphenylarsine, phenyl iodide, 1-chloro-4-iodobenzene, 1-methoxy-4-iodobenzene, tri-*n*-butyl(vinyl)tin and tri-*n*-butyltin iodide (Aldrich) were commercially available. Pd^0(dba)$_2$ was prepared according to a described procedure.[27]

General Procedure for Conductivity Measurements. In a cell thermostated at 25 °C containing 15 mL DMF was added successively 17 mg (0.03 mmol) Pd^0(dba)$_2$, 18.4 mg (0.06 mmol) AsPh$_3$ and 3.4 μL (0.03 mmol) PhI. The residual conductivity κ_0 (3 μS.cm^{-1}) was measured. 87 μL (0.3 mmol) CH$_2$=CH−Sn(*n*-Bu)$_3$ was then added and the conductivity recorded versus time using a computerized homemade program, until it reached a constant final value (Figure 1a).

[Ph$_2$Pd$_2$(μ^2-I)$_2$(AsPh$_3$)$_2$]. 100 mL of anhydrous THF was added to 1 g (1.74 mmol) of Pd(dba)$_2$, 0.532 g (1.74 mmol) of AsPh$_3$ and 0.39 mL (3.48 mmol) of PhI. After 2 h, THF was evaporated. After addition of ethyl ether, brown yellow crystals were collected 0.9 g (84% yield). Monocrystals were obtained by vapor diffusion from CH$_2$Cl$_2$/Et$_2$O. Anal. Calcd for C$_{48}$H$_{40}$-As$_2$I$_2$Pd$_2$: C, 46.7; H, 3.3. Found: C, 46.44; H, 3.35. ^{1}H NMR (250 MHz, CDCl$_3$, TMS): δ 6.63 (t, 1H, J = 7 Hz, *p*-H), 6.66 (t, 2H, J = 7 Hz, *m*-H), 7.10 (dd, 2H, J = 7 and 1.2 Hz, *o*-H), 7.26 (m, 6H, H of AsPh$_3$), 7.31 (t, 9H, H of AsPh$_3$) (addition of AsPh$_3$ into the NMR tube afforded the signals of PhPdI-(AsPh$_3$)$_2$ already reported).[8]

[PhPdI(AsPh$_3$)(DMF)] from [Ph$_2$Pd$_2$(μ_2−I)$_2$(AsPh$_3$)$_2$] (3 mM in DMF-d_7):^{1}H NMR (250 MHz, DMF-d_7, TMS): δ 6.62 (br s, $\Delta\nu_{1/2}$ = 14 Hz, 3H, *p*-H and *m*-H), 6.99 (br s, $\Delta\nu_{1/2}$ = 18 Hz, 2H, *o*-H), 7.43 (m, 15H, H of AsPh$_3$) (Figure 7a). Addition of 4 equivs AsPh$_3$ per dimer leads to the formation of pure PhPdI(AsPh$_3$)$_2$ with a well-defined spectrum (vide infra and Figure 7c).

[PhPdI(AsPh$_3$)$_2$][8] (4 mM in DMF-d_7) in the absence of AsPh$_3$: the signals of PhPdI(AsPh$_3$)$_2$ are not well resolved in DMF-d_7 due to its dynamic equilibrium with PhPdI(AsPh$_3$)-(DMF) and AsPh$_3$. ^{1}H NMR (250 MHz, DMF-d_7, TMS): δ 6.47 (m, 3H, *m*-H and *p*-H), 6.83 (m, 2H, *o*-H), 7.43 (m, 30 H, H of AsPh$_3$) (Figure 7b).

[PhPdI(AsPh$_3$)$_2$][8] (3 mM) in the presence of 6 equivs AsPh$_3$ or generated by addition of 5 equiv. AsPh$_3$ to the dimer [Ph$_2$Pd$_2$(μ_2–I)$_2$(AsPh$_3$)$_2$] in DMF-d_7: ^{1}H NMR (250 MHz, DMF-d_7): δ 6.37 (t, 2H, J = 7 Hz, *m*-H), 6.46 (t, 1H, J = 7 Hz, *p*-H), 6.78 (d, 2H, J = 7 Hz, *o*-H), 7.42 (s, H of AsPh$_3$) (Figure 7c).

[(*p*-MeO−C$_6$H$_4$)PdI(AsPh$_3$)$_2$]. 0.5 mL of CDCl$_3$ was added to 5.8 mg (0.01 mmol) of Pd(dba)$_2$ and 6 mg (0.02 mmol) of AsPh$_3$ followed by 2.3 mg (0.01 mmol) of *p*-MeO−C$_6$H$_4$–I. ^{1}H NMR (400 MHz, CDCl$_3$): δ 2.19 (s, 3H, C*H*$_3$), 6.07 (d, 2H, J = 8.7 Hz), 6.52 (d, 2H, J = 8.7 Hz), 7.30 (t, J = 7.5 Hz, *m*-H of AsPh$_3$), 7.38 (m, *p*-H of AsPh$_3$) 7.47 (m, *o*-H of AsPh$_3$). The ^{1}H NMR spectrum also exhibited the signals of the dimer **[(*p*-MeO−C$_6$H$_4$)$_2$Pd$_2$I$_2$(AsPh$_3$)$_2$]** (16% dissociation): δ 2.23 (s,

(25) In a real catalytic reaction where PhI is in large excess compared to the palladium catalyst, the half-reaction time of the oxidative addition will be considerably shorter than that (8 s) determined in the present work under stoichiometric conditions ([Pd^0] = [PhI] = 2 mM, vide supra). For example, for [Pd^0] = 2mM and [PhI] = 80 mM, $t_{1/2}$ = 0.2 s. However, in the presence of CH$_2$=CH−SnBu$_3$ (80 mM) (the highest concentration investigated in this work) the oxidative addition will be slower than that latter, with a half-reaction time of ca. 1s, as estimated from our previous work.[8] Nevertheless, this still corresponds to a very fast reaction in comparison to the rate of the overall catalytic reaction. Indeed, the reaction of CH$_2$=CH−SnBu$_3$ with PhPdI(AsPh$_3$)$_2$ (2 mM) investigated here was found to be slower than the oxidative addition performed under the catalytic conditions, i.e., in the presence of CH$_2$=CH−SnBu$_3$, since the fastest transmetalation, observed with CH$_2$=CH−SnBu$_3$ (80 mM), exhibited a half-reaction time of 9 s. These results confirm that the reaction of CH$_2$=CH−SnBu$_3$ with PhPdI(AsPh$_3$)$_2$ via PhPdI(AsPh$_3$)(DMF) is the rate determining step of the catalytic cycle also in DMF, as previously established by Farina[3] in THF, via the investigation of the kinetics of the catalytic reaction.

(26) This is an application of the steady-state approximation for a reactive moiety involved in a fast equilibrium with a non reactive species.

(27) Takahashi, Y.; Ito, Ts.; Ishii, Y. *J. Chem. Soc. Chem. Commun.* **1970**, 1065−1066.

3H, CH_3), 6.72 (d, 2H, $J = 9$ Hz), 7.60 (d, 2H, $J = 9$ Hz), 7.30 (t, $J = 7.5$ Hz, *m*-H of $AsPh_3$), 7.38 (m, *p*-H of $AsPh_3$) 7.47 (m, *o*-H of $AsPh_3$). The signals at 2.23, 6.72 and 7.60 ppm disappeared upon addition of $AsPh_3$ to afford only that of (*p*-MeO$-C_6H_4$)PdI$(AsPh_3)_2$ described just above.

[(*p*-Cl$-C_6H_4$)PdI$(AsPh_3)_2$]. 0.5 mL of $CDCl_3$ was added to 5.8 mg (0.01 mmol) of Pd(dba)$_2$ and 6 mg (0.02 mmol) of $AsPh_3$ followed by 2.4 mg (0.01 mmol) of *p*-Cl$-C_6H_4$-I. ^{1}H NMR (250 MHz, $CDCl_3$): δ 6.30 (d, 2H, $J = 8.4$ Hz), 6.55 (d, 2H, $J = 8.4$ Hz), 7.30−7.38 (m, H of $AsPh_3$), 7.40 (m, H of $AsPh_3$). The ^{1}H NMR spectrum also exhibited the signals of the dimer **[(*p*-Cl$-C_6H_4)_2Pd_2I_2(AsPh_3)_2$]** (18% dissociation)**:** δ 6.64 (d, 2H, $J = 8.4$ Hz), 6.99 (d, 2H, $J = 8.4$ Hz), 7.30−7.38 (m, H of $AsPh_3$), 7.40 (m, H of $AsPh_3$). The signals at 6.64 and 6.99 ppm disappeared upon addition of $AsPh_3$ to afford only that of (*p*-Cl$-C_6H_4$)PdI$(AsPh_3)_2$ described just above.

Acknowledgment. This work has been supported in part by the Centre National de la Recherche Scientifique (CNRS, UMR 8640 and 7653), the Ministère de la Recherche (Ecole Normale Supérieure) and the University Paris VI (UPMC). We thank the editor, the referees and Professor P. Espinet for the discussion about the existence of the dimer in chloroform. We thank Johnson Matthey for a generous loan of sodium tetrachloropalladate.

Supporting Information Available: Full details of the crystallographic analysis. This material is available free of charge via the Internet at http://pubs.acs.org.

JA0204978